Article

A Versatile Biosensing Platform for DNA Detection Based on a DNAzyme and Restriction-Endonuclease-Assisted Recycling

Ling Yuan, Wenwen Tu, Jianchun Bao, and Zhihui Dai

Anal. Chem., **Just Accepted Manuscript** • DOI: 10.1021/ac5034903 • Publication Date (Web): 10 Dec 2014

A Versatile Biosensing Platform for DNA Detection Based on a DNAzyme and Restriction-Endonuclease-Assisted Recycling

Ling Yuan,† Wenwen Tu,† Jianchun Bao and Zhihui Dai*

Jiangsu Collaborative Innovation Center of Biomedical Functional Materials and Jiangsu Key Laboratory of Biofunctional Materials, College of Chemistry and Materials Science, Nanjing Normal University, Nanjing, 210023, P. R. China

On the basis of a DNAzyme and a restriction-endonuclease-assisted target recycling strategy using Pd-Au alloy nanocrystals to immobilize probe DNA on an electrode and catalyze the reduction of H_2O_2 which amplified signal and promoted the detection sensitivity, a versatile biosensing platform for DNA detection was proposed. Using p53 and oral cancer genes as models, hemin/G-quadruplex simultaneously acted as a reduced nicotinamide adenine dinucleotide (NADH) oxidase and a horseradish peroxidase (HRP)-mimicking DNAzyme, and a versatile DNA biosensor was designed for the first time based on the good electrocatalytic activity of Pd-Au alloy nanocrystals. Hemin/G-quadruplex catalyzed the reduction of H_2O_2, which was generated from NADH in the presence of O_2, to produce an electrochemical signal when thionine functioned as the electron mediator. Moreover, the nicking endonuclease N.BstNB I caused the target DNA to cycle for multiple rounds and further amplified the electrochemical response. This versatile DNA biosensor exhibited linear ranges for the detection of p53 and oral cancer genes from 0.1 fmol L^{-1} to 0.1 nmol L^{-1} and 0.1 fmol L^{-1} to 1 nmol L^{-1}, respectively. The detection limits, established as 3σ, were estimated to be 0.03 fmol L^{-1} and 0.06 fmol L^{-1} for the p53 and oral cancer genes, respectively. The as-prepared biosensor could discriminate mismatched sequences, indicating a satisfactory selectivity and validating the feasibility of the proposed strategy. More importantly, simply by changing the helper DNA, this versatile DNA biosensor could detect different target DNA species, which could create a new avenue for the potential diagnosis of cancer.

DNA detection has attracted extensive attention because DNA species play an important role in clinical diagnosis and biomedical studies.[1-6] Therefore, there is an urgent need for the construction of a versatile DNA biosensor because of the ease of operation and cost-effectiveness of such tools. A biosensor has recently been fabricated to detect different target DNA species by changing the sequence of the capture and assistant strands.[7] In this work, a versatile and convenient biosensing platform for the detection of different DNA species was developed by simply changing the helper DNA. Recent studies have shown that hemin/G-quadruplex can act as a horseradish peroxidase (HRP)-mimicking DNAzyme and reduce nicotinamide adenine dinucleotide (NADH) oxidase to detect many biomolecules, such as proteins and DNA.[8-14] First, the hemin/G-quadruplex acted as an NADH oxidase, aiding the oxidation of NADH to the cofactor NAD^+ with the concomitant formation of H_2O_2. Subsequently, using thionine as an electron mediator, hemin/G-quadruplex catalyzed the reduction of H_2O_2 to generate an electrochemical signal.[13] According to this principle, a versatile and convenient biosensing platform for DNA detection based on hemin/G-quadruplex, which simultaneously acted as a NADH oxidase and a HRP-mimicking DNAzyme, was constructed for the first time in this work. This platform avoided labeling the DNA with protein enzymes or catalytic metals and reduced the interference of dissolved oxygen.

Due to its easy operation, high sensitivity and selectivity, the electrochemical detection of DNA species has attracted extensive attention.[15-17] To improve the sensitivity of DNA detection, different approaches have been adopted to amplify the signal, including utilizing labeled nanoparticles[18-20] combining with polymerase chain reaction,[21] circular rolling circle amplification[22] and hybridization chain reaction.[23] However, these above approaches are often time-consuming, costly or complex.[24]

Nucleases such as restriction endonucleases and exonuclease III have been used to amplify the signal due to their easy operation and time savings.[25-26] Unlike exonuclease III, restriction endonucleases can only cleave specific sites because they recognize a specific sequence in double-stranded DNA (dsDNA),[27-30] which makes the DNA detection more precise and specific. Nicking endonuclease N.BstNB I, a restriction endonuclease, recognizes a sequence (5′-GAGTC-3′) that contains the complementary sequence of the p53 and oral cancer genes.[31,32] Highly sensitive detection of the p53 gene, which is a tumor suppressor and is known as "the guardian of genome",[33,34] and the oral cancer gene is beneficial for the early diagnosis of cancer. Therefore, N.BstNB I was used to amplify the electrochemical signal to improve the detection sensitivity of p53 and oral cancer genes in this work.

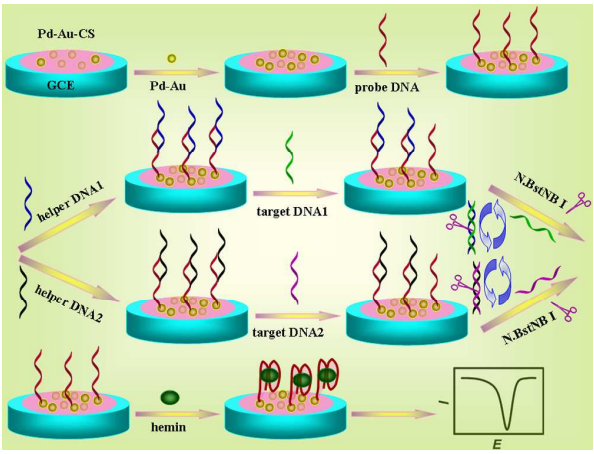

Scheme 1. A schematic illustration of the versatile biosensing platform for the detection of DNA.

Pd-Au alloy nanocrystals (NCs), as one type of bimetallic nanomaterial, have received considerable attention for their unique catalytic properties, which are very different from those of their monometallic NC components.[35-37] Due to the presence of an atomic ensemble and the effective electronic coupling effects of their constituents, Pd-Au alloy NCs exhibit enhanced catalytic activities compared with

pure Pd NCs and Au NCs.[38-41] As a result of their excellent properties, Pd-Au alloy NCs, which can also catalyze the reduction of H_2O_2[42] and immobilize probe DNA onto the electrode, were adopted to fabricate a versatile biosensing platform in this work. The versatile biosensing platform for the determination of different DNA species was constructed based on a DNAzyme and a restriction-endonuclease-assisted target recycling strategy (Scheme 1). Notably, at a negative potential scanning from -0.5-0 V, the negatively charged electric field of the electrode surface reoriented the negatively-charged oligonucleotide perpendicular to the electrode surface rather than lay flat on the electrode, due to the static repulsion force.[43,44] First, probe DNA was immobilized on Pd-Au alloy NCs, and then, helper DNA was partially hybridized with the probe DNA. Subsequently, the target DNA mostly hybridized with helper DNA to form a sequence of dsDNA,[45] which departed from the electrode. Meanwhile, part of the probe DNA became single-stranded again. N.BstNB I recognized the specific sequence in the dsDNA and cleaved the fragment of helper DNA. After that, the target DNA became single-stranded and hybridized once more with the helper DNA on the electrode surface to make more probe DNA become single-stranded. In this way, the released target DNA could hybridize with un-nicked helper DNA and facilitate a new cycle of single-stranded probe DNA. Finally, the single-stranded probe DNA reacted with hemin and to form hemin/G-quadruplex. Pd-Au alloy NCs and the hemin/G-quadruplex catalyzed the reduction of H_2O_2, which was generated from NADH in the presence of O_2. Using thionine as an electron mediator, an electrochemical signal was obtained. In the presence of G-quadruplex DNAzyme, by Pd-Au NCs catalyzing the reduction of H_2O_2, the electrochemical response was further enhanced which amplified signal, leading to the promotion of detection sensitivity. By changing the helper DNA, different target DNA could be detected

using this designed strategy. Herein, a versatile biosensing platform is proposed.

EXPERIMENTAL SECTION

Reagents and Materials. Tris (2-carboxyethyl) phosphine hydrochloride (TCEP), tris (hydroxymethyl) aminomethane, 3-mercapto-1-hexanol (MCH), reduced NADH, chitosan (CS) and $HAuCl_4$ were purchased from Sigma-Aldrich. Hemin, thionine (TH), dodecylamine (DDA) and 1-octadecene (ODE) were purchased from Alfa Aesar. N.BstNB I and NEBuffer 3 were purchased from New England BioLabs. Dimethyl sulfoxide (DMSO), ethylenediamine tetraacetic acid (EDTA), $Pd(NO_3)_2$, NaCl, NaH_2PO_4 and Na_2HPO_4 were obtained from the Sinopharm Chemical Reagent Co., Ltd. The stock solution of hemin (1 mmol L^{-1}) was prepared in DMSO, stored at -20 °C and diluted to the required concentrations with Tris-HCl buffer solution. The 10 mmol L^{-1} TE buffer (pH = 7.4) consisted of 10 mmol L^{-1} Tris-HCl and 1 mmol L^{-1} EDTA. The 10 mmol L^{-1} PB buffer (pH = 7.4) was a mixture of 10 mmol L^{-1} NaH_2PO_4 and 10 mmol L^{-1} Na_2HPO_4. The DNA immobilization buffer consisted of 10 mmol L^{-1} TE buffer, 1000 mmol L^{-1} NaCl and 10 mmol L^{-1} TCEP. The hybridization buffer consisted of 100 mmol L^{-1} NaCl and 10 mmol L^{-1} TE buffer. The washing buffer solution was a mixture of 10 mmol L^{-1} PB buffer and 100 mmol L^{-1} NaCl. All other chemicals were of analytical grade. All of the aqueous solutions were prepared with doubly distilled water (DDW). The DNA strands were prepared and purified using a high-performance liquid chromatograph from Sangon Biotech (Shanghai) Co., Ltd, and their base sequences are listed as follows.

Probe DNA: 5′-TCTTTGGGTTGGGCGGGATGGGTCATT-$(CH_2)_3$-SH-3′ (DNA1)

Helper DNA1: 5′-ACCCAAAGAGTCTTCCAGTGTGATGA-3′ (DNA2)

Target DNA1 (p53): 5′-TCATCACACTGGAAGACTC-3′ (DNA3)

Mismatch1: 5′-TCATCACA***A***TGGAAGACTC-3′ (DNA4)

Mismatch2: 5′-TCATCACACTGGAA***T***ACTC-3′ (DNA5)

Mismatch3: 5′-TCATCACACTGGA***TC***ACTC-3′ (DNA6)

Helper DNA2: 5′-ACCCAAAGAACGAGAGTCTTTCTG-3′ (DNA22)

Target DNA2 (oral cancer): 5′-CAGAAAGACTCTCGTTCTTT-3′ (DNA33)

Mismatch11: 5′-CA***C***AAAGACTCTCGTTCTTT-3′ (DNA44)

Mismatch22: 5′-CAGAAA***C***ACTCTCGTTCTTT-3′ (DNA55)

Mismatch33: 5′-CAGAAAGACT***AG***CGTTCTTT-3′ (DNA66)

Apparatus and Measurements. Differential pulse voltammetry (DPV) was performed on a CHI 660D electrochemical workstation (CH Instruments Inc., USA). The potential scanning range was -0.5-0 V, and the amplitude was 50 mV. Electrochemical impedance spectra (EIS) were collected on an Autolab PGSTAT302N potentiostat/galvanostat (Eco Chemie B.V., The Netherlands). The EIS experiments were carried out under open-circuit conditions, with frequencies ranging from 0.1 Hz to 10^5 Hz and an AC voltage amplitude of 5 mV. The supporting electrolyte was a solution of 5 mmol L^{-1} $K_3[Fe(CN)_6]$ and 5 mmol L^{-1} $K_4[Fe(CN)_6]$ (1:1) containing 0.1 mol L^{-1} KCl. The three-electrode electrochemical system consisted of a saturated calomel electrode as the reference electrode, a platinum wire as the auxiliary electrode and a bare or modified glassy carbon electrode (GCE) (d = 3 mm) as the working electrode. Transmission electron microscopy (TEM) images were recorded on a JEM-200CX instrument (Japan) at an acceleration voltage of 200 kV. High resolution transmission electron microscopy (HRTEM) images were collected with a JEOL-2100F apparatus using an acceleration voltage of 200 kV. Energy dispersive spectra (EDS) were acquired with a JSM-5610LV-Vantage energy spectrometer. X-ray diffraction (XRD) patterns were characterized in a powder sample using a D/max

2500VL/PC diffractometer (Japan) equipped with a graphite monochromator and Cu Kα radiation (λ = 1.54060 Å).

Synthesis of the Pd-Au Alloy NCs. The synthesis recipe used to prepare the Pd-Au alloy NCs was developed by our lab. $Pd(NO_3)_2$ (0.115 g, 0.5 mmol), DDA (3 mL) and ODE (5 mL) were added to a 250 mL three-neck flask at room temperature. Then, the reactor was heated from room temperature to 250 ℃ at a rate of 7-8 ℃ min^{-1} and held at 250 ℃ for 5 minutes. After that, $HAuCl_4$ solution was quickly added to the reaction system, which was kept at 250 ℃ for another 15 minutes. The $HAuCl_4$ solution was prepared by dissolving 0.205 g of $HAuCl_4$ (0.5 mmol) in a mixture of 5 mL ODE and 3 mL DDA. Finally, the reactor was cooled to room temperature naturally. After collecting and washing the crude product with heptane and absolute ethanol several times to remove by-products, the precipitate was centrifuged and dried to obtain Pd-Au alloy NCs for further characterization and analysis.

Preparation of the Pd-Au-CS and Pd-Au Suspension. One milligram of CS was transferred into 4 mL of 1% acetic acid solution and then ultrasonicated to obtain a uniform CS solution. Next, 5 mg of Pd-Au alloy NCs was added into 1 mL of CS solution and ultrasonicated to obtain a uniform Pd-Au-CS suspension. A total of 5 mg of Pd-Au alloy NCs was added into 1 mL of an ethanol-water (V/V, 1:2) solution, and the mixture was then ultrasonicated to obtain a uniform Pd-Au suspension.

Preparation of the Biosensor. The GCE was successively polished with 1.0, 0.3, and 0.05 μm $\alpha-Al_2O_3$ powder. After sonication in water, the electrode was rinsed with DDW and allowed to dry under a stream of nitrogen gas. A 6 μL aliquot of the Pd-Au-CS suspension was dropped onto the pretreated GCE and dried to obtain GCE/Pd-Au-CS. Then, 6 μL of the Pd-Au suspension was dropped onto GCE/Pd-Au-CS and dried to obtain GCE/Pd-Au-CS/Pd-Au. Following a rinse with

washing buffer and DDW, 6 μL of probe DNA (DNA1, 1 μmol L^{-1}) was dropped onto GCE/Pd-Au-CS/Pd-Au and held at 4 °C overnight to obtain GCE/Pd-Au-CS/Pd-Au/DNA1. Subsequently, 6 μL of MCH (1 mol mL^{-1}) was dropped onto GCE/Pd-Au-CS/Pd-Au/DNA1 after washing with washing buffer and DDW, and the electrode was incubated for an hour to obtain GCE/Pd-Au-CS/Pd-Au/DNA1/MCH. After that, helper DNA (DNA2 or DNA22, 1 μmol L^{-1}) was dropped onto GCE/Pd-Au-CS/Pd-Au/DNA1/MCH, and then the electrode was washed and incubated for one hour at 37 °C to obtain GCE/Pd-Au-CS/Pd-Au/DNA1/MCH/DNA2(DNA22). Next, 8 μL of target DNA (DNA3 or DNA33) at different concentrations was dropped onto GCE/Pd-Au-CS/Pd-Au/DNA1/MCH/DNA2(DNA22), after which the electrode was washed and incubated for one hour at 37 °C. Afterward, the modified electrode was incubated in NEBuffer containing 10 units/μL N.BstNB I at 55 °C and washed with washing buffer and DDW. Finally, the electrode was incubated in a hemin (2 μmol L^{-1}) solution for one hour to form the hemin/G-quadruplex DNAzyme at room temperature. The different electrodes were used for continuous hybridization of target DNA from low concentration to high value. Prior to performing the electrochemical detection, the system needed deaeration with nitrogen for 20 min, which avoided the oxidation of thionine. During the entire process of electrochemical detection, it did not need to deaerate with nitrogen or keep over a N_2 atmosphere because a small amount of O_2 was needed to participate the reaction of forming H_2O_2 which was generated from NADH in this system.

RESULTS AND DISCUSSION

Characterization of the Pd-Au Alloy NCs. Figure 1A showed the EDS pattern of the Pd-Au alloy NCs synthesized in our lab. Except for the small C peak, which was

generated from the surface adsorbed organic reagents, only two types of metallic elements, namely Pd and Au, were observed in the sample. The atomic number ratio of Pd and Au approached 1:4 by integral calculation, suggesting that the sample might be $PdAu_4$ alloy NCs. Further evidence was provided from the XRD analysis (Figure 1B). In the $30 < 2\theta < 85^{o}$ range, five obvious diffraction peaks were observed in the obtained Pd-Au alloy NCs, indicating that the sample was well-crystallized. Furthermore, the positions of those five diffraction peaks were located between those of pure face-centered cubic phase (*fcc*) Pd NCs and *fcc* Au NCs, demonstrating that the obtained sample was Pd-Au alloy NCs and that their phase structure was still *fcc*. According to Vegard's law, the weight percents of Pd and Au in this alloy sample were approximately 20% and 80%, respectively, which were calculated from the XRD pattern. Based on the analysis of the EDS and XRD patterns, the sample obtained under typical conditions was $PdAu_4$ alloy NCs.

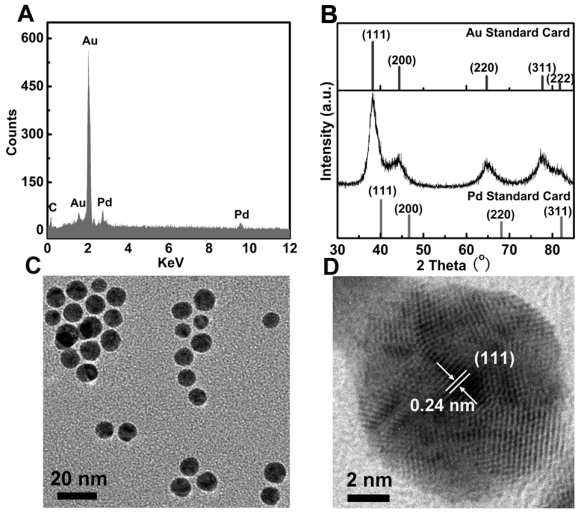

Figure 1. EDS (A) and XRD (B) patterns of Pd-Au alloy NCs obtained under the typical synthetic conditions; TEM image (C) and HRTEM image (D) of Pd-Au alloy NCs.

The morphologies of the Pd-Au alloy NCs were examined by TEM. Figure 1C

displays the low-magnification TEM image obtained. $PdAu_4$ alloy NCs were nearly monodispersed and quasi-spherical, and the average size was estimated to be 8 nm. Corresponding HRTEM analysis (Figure 1D) displayed clear and continuous lattice fringes. The lattice spacing was measured to be approximately 2.4 Å, which falls between the interplanar separation of the (111) plane of *fcc* Pd and the (111) plane of *fcc* Au. These results indicated that the surfaces of $PdAu_4$ alloy NCs were dominated by (111) planes and further confirmed that the obtained sample was a nanoalloy with high crystallinity. Pd and Au NCs were also synthesized, and the corresponding characterizations are shown in Figures S1-S2 of the Supporting Information.

Electrochemical Behavior. Figure 2 shows the DPVs of different modified electrodes in 10 mmol L^{-1} Tris-HCl solution containing 1.5 mmol L^{-1} NADH and 30 μmol L^{-1} thionine. A small current was obtained for GCE/Pd-Au-CS/Pd-Au/DNA1/MCH/DNA2 (curve a). In the presence of hemin and N.BstNB I but without target DNA (curve b), or in the presence of N.BstNB I and 1×10^{-12} mol L^{-1} target DNA but without hemin (curve c), there were no significant changes in the peak DPV currents compared with curve a, suggesting that hemin/G-quadruplex was not formed. In the absence of target DNA, probe DNA, which contained a large number of G bases, could not become single-stranded to react with hemin and form hemin/G-quadruplex. Additionally, hemin/G-quadruplex cannot form without hemin, even if the probe DNA is a single strand. In the absence of hemin/G-quadruplex, H_2O_2, which was generated from NADH in the presence of O_2, could not be produced, as a result of which, the electrochemical responses did not obviously change after using thionine as an electron mediator.

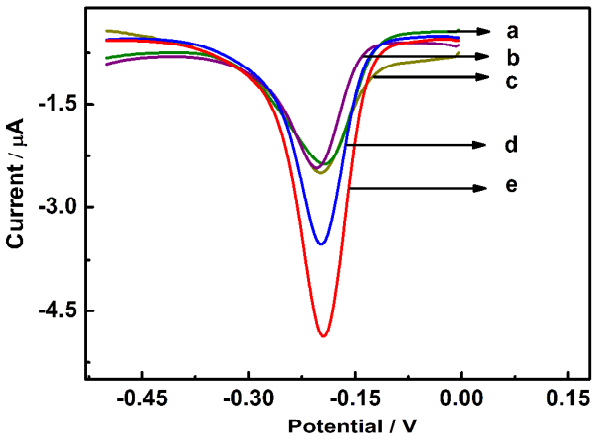

Figure 2. DPVs of GCE/Pd-Au-CS/Pd-Au/DNA1/MCH/DNA2 in the absence of target DNA, N.BstNB I and hemin (a), in the presence of hemin and N.BstNB I but without target DNA (b), in the presence of N.BstNB I and 1×10^{-12} mol L^{-1} target DNA but without hemin (c), in the presence of 1×10^{-12} mol L^{-1} target DNA and hemin but without N.BstNB I (d), and in the presence of 1×10^{-12} mol L^{-1} target DNA, N.BstNB I and hemin (e) in a 10 mmol L^{-1} Tris-HCl solution containing 1.5 mmol L^{-1} NADH and 30 μmol L^{-1} thionine.

With hemin and 1×10^{-12} mol L^{-1} target DNA but without N.BstNB I, there was a visible increase in the peak DPV current (curve d). When the probe DNA became single-stranded and the hemin/G-quadruplex formed, the DPV peak current was enhanced. After adding N.BstNB I, the nicking reaction happened, and the peak DPV current increased significantly (curve e), indicating that a large amount of hemin/G-quadruplex formed with the help of the nicking endonuclease N.BstNB I. Therefore, N.BstNB I was adopted in this system for signal amplification.

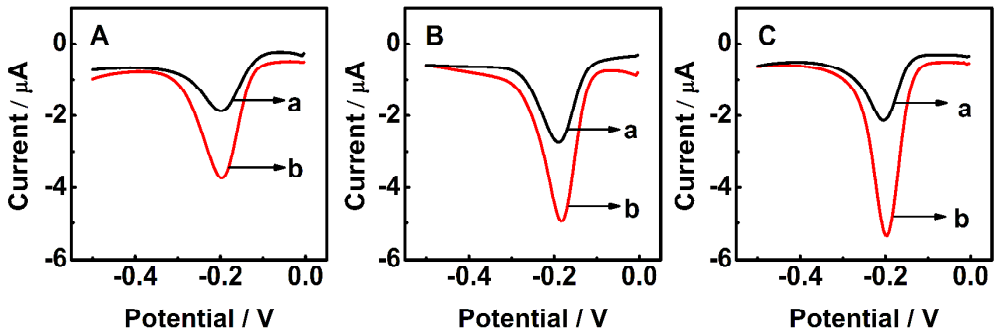

Figure 3. DPVs of different modified electrodes without target DNA (curve a) and with 1×10^{-11} mol L^{-1} target DNA (curve b) in the presence of hemin and N.BstNB I. The different modified electrodes were as follows: GCE/Pd-CS/Pd/DNA1/MCH/DNA2 (A), GCE/Au-CS/Au/DNA1/MCH/DNA2 (B) and GCE/Pd-Au-CS/Pd-Au/DNA1/MCH/DNA2 (C), respectively.

The DPVs of different modified electrodes in a 10 mmol L^{-1} Tris-HCl solution containing 1.5 mmol L^{-1} NADH and 30 μmol L^{-1} thionine are displayed in Figure 3. Curve a in Figures 3A-3C shows the DPVs of GCE/Pd-CS/Pd/DNA1/MCH/DNA2, GCE/Au-CS/Au/DNA1/MCH/DNA2, and GCE/Pd-Au-CS/Pd-Au/DNA1/MCH/DNA2 in the presence of hemin and N.BstNB I but without target DNA. Curve b in Figures 3A-3C shows the DPVs of GCE/Pd-CS/Pd/DNA1/MCH/DNA2, GCE/Au-CS/Au/DNA1/MCH/DNA2, and GCE/Pd-Au-CS/Pd-Au/DNA1/MCH/DNA2 in the presence of hemin, N.BstNB I and 1×10^{-11} mol L^{-1} target DNA. It was obvious that the difference between the peak currents of curve a and curve b in Figure 3C was the largest, which indicated that the Pd-Au alloy NCs possessed a better electrochemical response than Pd NCs (Figure S1**)** and Au NCs (Figure S2). This enhancement of the signal may be caused by two alloy effects, i.e., ensemble and ligand effects.[38,39] Moreover, EIS were performed to further explain why the best response of Pd-Au NCs was obtained (Figure S3 of the Supporting Information).

Comparing with that of GCE/Pd-CS/Pd (curve a) and GCE/Au-CS/Au (curve b), the electron-transfer resistance (R_{et}) of GCE/Pd-Au-CS/Pd-Au (curve c) was lowest, indicating that Pd-Au more effectively facilitated electron transportation and reduced surface diffusion capacitance between the redox probe and the electrode surface than those of the two others. More importantly, this phenomenon suggested Pd-Au NCs much more decreased the steric hindrances for redox probe to the electrode surface than those of the two others, which may be more beneficial for NADH and H_2O_2 diffusion to the electrode surface, leading to the best response. Thus, the electrochemical response of the Pd-Au alloy NCs showed enough sensitivity for the development of a versatile biosensing platform to detect DNA.

The comparison of the DPVs responses using Pd-Au and Pd-Au-CS/Pd-Au modified electrodes was performed to explain why we assembled the electrode first with Pd-Au-CS then Pd-Au NCs (Figure S4 of the Supporting Information). Compared with that of GCE/Pd-Au/DNA1/MCH/DNA2 (Figure S4A, curve b), the electrochemical response of GCE/Pd-Au-CS/Pd-Au/DNA1/MCH/DNA2 towards 1×10^{-11} mol L^{-1} target DNA dramatically promoted (Figure S4B, curve b). The increased current $\triangle I$ ($\triangle I = I_0$-I; the current response recorded as I_0 when the target DNA concentration was zero; I was the current of 1×10^{-11} mol L^{-1} target DNA) was 2.32-fold higher than that of GCE/Pd-Au/DNA1/MCH/DNA2. Thus, the electrode first with Pd-Au-CS then Pd-Au NCs had the better performance.

Characterization of the Biosensor Fabrication Process. EIS was used to confirm the biosensor construction process (Figure 4). After the electrode was modified with Pd-Au-CS (curve b), the semicircle domain became smaller compared with that of the bare GCE (curve c). When Pd-Au was added to the surface of GCE/Pd-Au-CS (curve a), the semicircle domain further decreased, suggesting that

Pd-Au had been immobilized onto the electrode surface. Pd-Au accelerated the electron transfer between the redox probe and the electrode surface due to its good electronic conductivity. After DNA1 was added to the surface of GCE/Pd-Au-CS/Pd-Au (curve d), the electron-transfer resistance (R_{et}) increased, indicating that DNA1 had been successfully grafted onto the electrode surface, which hindered the electron transfer. Next, MCH was added to GCE/Pd-Au-CS/Pd-Au/DNA1, and a further increase of R_{et} was observed (curve e), suggesting that MCH had been successfully immobilized onto the electrode surface as a blocking reagent. Subsequently, when DNA2 was added to the surface of GCE/Pd-Au-CS/Pd-Au/DNA1/MCH (curve g), the semicircle domain became larger compared with that of GCE/Pd-Au-CS/Pd-Au/DNA1/MCH (curve e), demonstrating that DNA2 had been partly hybridized with DNA1 and formed dsDNA, which contained a more negative charge. The increased R_{et} might be attributed to the fact that the negative charges of the dsDNA phosphate backbone resisted the transfer of the negatively charged probe ($[Fe(CN)_6]^{3-/4-}$).

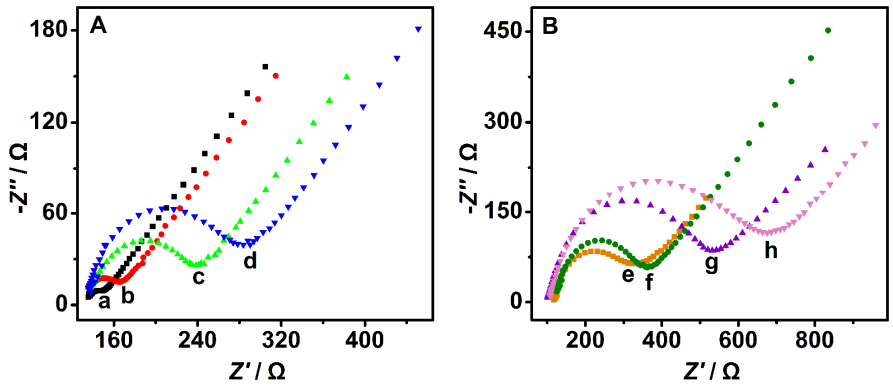

Figure 4. (A) EIS of GCE/Pd-Au-CS/Pd-Au (a), GCE/Pd-Au-CS (b), bare GCE (c), GCE/Pd-Au-CS/Pd-Au/DNA1 (d); (B) EIS of GCE/Pd-Au-CS/Pd-Au/DNA1/MCH (e), GCE/Pd-Au-CS/Pd-Au/DNA1/MCH/DNA2 in the presence of 1×10^{-12} mol L^{-1} DNA3 and N.BstNB I (f), GCE/Pd-Au-CS/Pd-Au/DNA1/MCH/DNA2 (g), and the

modified curve f electrode in the presence of hemin (h) in a 5 mmol L^{-1} $K_3Fe(CN)_6/K_4Fe(CN)_6$ (1:1) solution containing 0.1 mol L^{-1} KCl. The frequencies ranged from 0.1 Hz to 10^5 Hz, and the AC voltage amplitude was 5 mV.

After GCE/Pd-Au-CS/Pd-Au/DNA1/MCH/DNA2 was incubated with 1×10^{-12} mol L^{-1} DNA3 and N.BstNB I, the R_{et} decreased dramatically (curve f), which indicated that most of the double-stranded DNA became single-stranded probe DNA again. Finally, the above electrode was incubated with hemin and the R_{et} increased (curve h), suggesting that hemin had been successfully inserted into the probe DNA and formed a stable hemin/G-quadruplex. The formed hemin/G-quadruplex increased the steric hindrance and hindered the electron transfer of $[Fe(CN)_6]^{3-/4-}$, leading to an increase of impedance. These changes in the electron transfer resistance verified the successful fabrication of the DNA biosensor.

The Mechanism of the Produced Electrochemical Signal. The detailed mechanism of the electrochemical signal produced can be described as follows:[12,13]

$Fe(III) + NADH \rightarrow Fe(II) + NAD^{\bullet} + H^{+}$ (1)

$Fe(II) + NAD^{\bullet} + H^{+} + O_2 \rightarrow NAD^{+} + Fe(III)–OOH$ (2)

$Fe(III)–OOH + H^{+} \rightarrow H_2O_2 + Fe(III)$ (3)

$H_2O_2 + Fe(III) \rightarrow Fe(II) + H_2O$ (4)

$Fe(II) + TH \rightarrow Fe(III) + TH^{+}$ (5)

$TH^{+} + H^{+} + 2e \rightarrow TH_2$ (6)

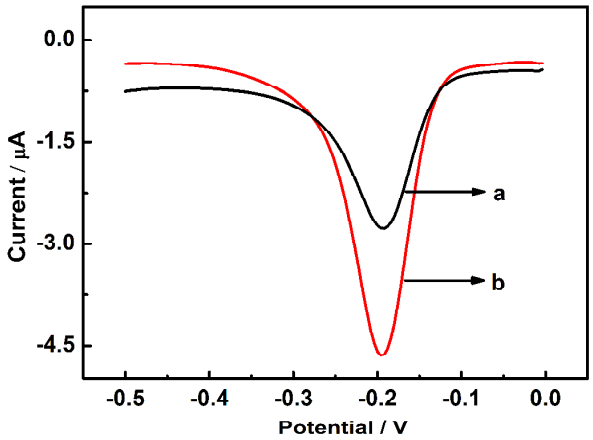

Figure 5. DPVs of GCE/Pd-Au-CS/Pd-Au/DNA1/MCH/DNA2 in the presence of 1×10^{-12} mol L^{-1} target DNA, N.BstNB I and hemin without NADH (a), and with 1.5 mmol L^{-1} NADH (b) in a 10 mmol L^{-1} Tris-HCl solution containing 30 μmol L^{-1} thionine.

First, NADH in the electrolytic cell participated in reactions (1) and (2) with the hemin/G-quadruplex first acting as an NADH oxidase and helping the oxidation of NADH to cofactor NAD^+. Then, reaction (3) occurred, and H_2O_2 was produced in the presence of dissolved O_2, which decreased the interference of O_2 in DNA determination. Subsequently, hemin/G-quadruplex acted as an HRP-mimicking DNAzyme and catalyzed the reduction of H_2O_2 to produce an electrochemical signal when thionine functioned as an electron mediator. This mechanism was also demonstrated in experiments in this work. As shown in Figure 5, the electrochemical response of the modified electrode with 1.5 mmol L^{-1} NADH (curve b) was much larger than that without NADH (curve a) in a 10 mmol L^{-1} Tris-HCl solution containing 30 μmol L^{-1} thionine. The reason for this is that reactions (1)-(3) took place when NADH was present, and after that, reactions (4)-(6) occurred, generating the electrochemical signal.

Versatile Biosensing Platform for the Detection of p53 and Oral Cancer Genes. Under optimal conditions (Figure S5 of the Supporting Information), the responses of the biosensor towards different concentrations of p53 and oral cancer genes are displayed in Figures 6 and Figure S6 of the Supporting Information. The p53 gene plays key roles in many cellular anti-cancer mechanisms and controls the level of reactive oxygen species. The p53 gene is activated and organizes cellular responses including cell cycle arrest, apoptosis and DNA repair when the organism is exposed to stress signals, such as hypoxia and DNA damage.[46-49] The DPV curves in Figure 6 show that the peak current gradually increased with increasing concentrations of the p53 gene (DNA3). This increase could be attributed to the fact that the presence of more target DNA caused more probe DNA to become single-stranded, after which the single-stranded probe DNA formed more hemin/G-quadruplex, enhancing the peak current. The calibration curve made by plotting ΔI ($\Delta I = I_0 - I$; the current response recorded as I_0 when the target DNA concentration was zero; I was the current of target DNA at different concentrations.) versus different p53 gene concentrations is shown in the inset of Figure 6. It was found that ΔI had a linear dependence on the logarithmic concentration of the p53 gene from 0.1 fmol L^{-1}–0.1 nmol L^{-1}. This linear range was wider than those of some other methods and modified electrodes[50-52] (Table S1 of the Supporting Information). The regression equation can be expressed as ΔI (μA) = 8.622 + 0.507 log$C$ (mol L^{-1}), and the regression coefficient (γ) was 0.9997. The detection limit was estimated to be 0.03 fmol L^{-1}, determined as 3σ (where σ is the relative standard deviation of 10 parallel measurements when the target DNA concentration was zero), which was lower than the detection limits of some other methods and modified electrodes[51-53] (Table S2 of the Supporting Information).

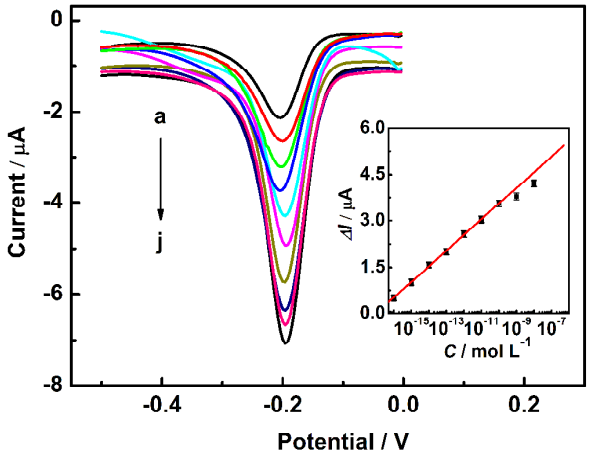

Figure 6. DPVs for different concentrations of the p53 gene in a 10 mmol L^{-1} Tris-HCl solution containing 1.5 mmol L^{-1} NADH and 30 μmol L^{-1} thionine. The concentrations of the p53 gene were 0 (a), 10^{-16} (b), 10^{-15} (c), 10^{-14} (d), 10^{-13} (e), 10^{-12} (f), 10^{-11} (g), 10^{-10} (h), 10^{-9} (i) and 10^{-8} mol L^{-1} (j). The inset is the corresponding calibration curve.

Because the oral cancer gene contained the complementary sequence of 5′-GAGTC-3′, which was recognized by the nicking endonuclease N.BstNB I, if the helper DNA was changed from DNA2 to DNA22, then the oral cancer gene (DNA33), which acted as the target DNA, could be detected by this method. When GCE/Pd-Au-CS/Pd-Au/DNA1/MCH/DNA22 was incubated with DNA33, N.BstNB I and hemin, a biosensor that could detect the oral cancer gene in a 10 mmol L^{-1} Tris-HCl solution containing 1.5 mmol L^{-1} NADH and 30 μmol L^{-1} thionine was achieved. The corresponding DPVs are shown in Figure S6 of the Supporting Information. The results show that the peak current gradually increased with increasing concentrations of the oral cancer gene. The calibration curve is displayed in the inset of Figure S6 of the Supporting Information. It was found that ΔI had a linear dependence on the logarithmic concentration of the oral cancer gene from 0.1 fmol L^{-1}–1 nmol L^{-1}. This linear range was wider than the 0.08 fmol L^{-1}–8 fmol L^{-1} range

detected by another modified electrode.[54] The regression equation was expressed as ΔI (μA) = 10.487 + 0.621 log$C$ (mol L^{-1}), and the regression coefficient (γ) was 0.9982. The detection limit was estimated to be 0.06 fmol L^{-1}, based on 3σ. Therefore, this designed versatile biosensing platform based on a DNAzyme and restriction endonuclease-assisted recycling exhibited a wide linear response range and high sensitivity in the determination of DNA.

Moreover, the proposed biosensor possessed mismatch discrimination ability and resisted interference in the determination of p53 gene and oral cancer gene (Figures S7-S8 of the Supporting Information), which indicated a satisfactory selectivity of the as-prepared DNA biosensor and validated the feasibility of the proposed strategy.

CONCLUSION

A versatile biosensing platform for the determination of different DNA species was developed based on a DNAzyme and a restriction endonuclease-assisted target recycling strategy. Pd-Au alloy NCs were facilely prepared and applied toward immobilizing probe DNA on the electrode, as well as catalyzing the reduction of H_2O_2. The alloy effects of the Pd-Au alloy NCs, such as ensemble and ligand effects, greatly improved their electrocatalytic activity compared with monometallic NC components. In the presence of G-quadruplex DNAzyme, by Pd-Au NCs catalyzing the reduction of H_2O_2, the electrochemical response was enhanced which amplified the signal for DNA detection. Using p53 and oral cancer genes as models, hemin/G-quadruplex acted as an NADH oxidase and HRP-mimicking DNAzyme at the same time, and the versatile DNA biosensor was constructed. Changes in the electron transfer resistance verified the successful fabrication of the DNA biosensor. Nicking endonuclease N.BstNB I caused the target DNA cycle to persist for multiple

rounds and further amplified the electrochemical response, thus enhancing the detection sensitivity. The biosensor exhibited good analytical performance, such as a low detection limit, wide linear range and satisfactory selectivity, validating the feasibility of the proposed strategy. By changing the helper DNA or nicking endonuclease, or the pretreatment of linking GAGTC sequence on different genes, this versatile biosensing platform could be applied for the determination of different DNA species and may have promising prospects for the early diagnosis of cancer.

ASSOCIATED CONTENT

Supporting Information Available

This information is available free of charge via the Internet at http://pubs.acs.org/.

AUTHOR INFORMATION

Corresponding Author

*Phone/Fax: +86-25-85891051; E-mail: daizhihuii@njnu.edu.cn

Author Contributions

[†]Ling Yuan and Wenwen Tu contributed equally to this work.

Notes

The authors declare no competing financial interest.

ACKNOWLEDGMENTS

This research was financially supported by the National Natural Science Foundation of China for the project (21175069, 21475062 and 21205061), Natural Science Foundation of Jiangsu (BK2012448), and Foundation of the Jiangsu Education Committee (11KJA150003 and 12KJB150016). We appreciate the financial support from the Priority Academic Program Development of Jiangsu Higher Education

Institutions and the Program for Jiangsu Collaborative Innovation Center of Biomedical Functional Materials.

REFERENCES

(1) Huang, J.; Wu, Y.; Chen, Y.; Zhu, Z.; Yang, X.; Yang, C. J.; Wang, K.; Tan, W. *Angew. Chem., Int. Ed.* **2011**, *50*, 401-404.

(2) Sassolas, A.; Leca-Bouvier, B. D.; Blum, L. J. *Chem. Rev.* **2008**, *108*, 109-139.

(3) Furst, A.; Landefeld, S.; Hill, M. G.; Barton, J. K. *J. Am. Chem. Soc*. **2013**, *135*, 19099-19102.

(4) Su, S.; Fan, J.; Xue, B.; Yuwen, L.; Liu, X.; Pan, D.; Fan, C.; Wang, L. *ACS Appl. Mater. Interfaces* **2014**, *6*, 1152-1157.

(5) Wang, Z.; Zhang, J.; Zhu, C.; Wu, S.; Mandler, D.; Marks, R. S.; Zhang, H. *Nanoscale* 2**014**, *6*, 3110-3115.

(6) Ferguson, B. S.; Buchsbaum, S. F.; Swensen, J. S.; Hsieh, K.; Lou, X.; Soh, H. T. *Anal. Chem.* **2009**, *81*, 6503-6508.

(7) Wang, Q.; Yang, L.; Yang, X.; Wang, K.; He, L.; Zhu, J.; Su, T. *Chem. Commun.* 2012, *48*, 2982-2984.

(8) Xiao, Y.; Rowe, A. A.; Plaxco. K. W. *J. Am. Chem. Soc.* **2007**, *129*, 262-263.

(9) Wang, F.; Elbaz, J.; Orbach, R.; Magen, N.; Willner, I. *J. Am. Chem. Soc.* **2011**, *133*, 17149-17151.

(10) Shimron, S.; Wang, F.; Orbach, R.; Willner, I. *Anal Chem.* **2012**, *84*, 1042-1048.

(11) Freeman, R.; Liu, X.; Willner, I. *J. Am. Chem. Soc.* **2011**, *133*, 11597-11604.

(12) Golub, E.; Freeman, R.; Willner, I. *Angew. Chem. Int. Ed.* **2011**, *50*, 11710-11714.

(13) Yuan, Y.; Yuan, R.; Chai, Y.; Zhuo, Y.; Ye, X.; Gan, X.; Bai, L. *Chem.*

Commun. **2012**, *48*, 4621-4623.

(14) Lu, L. M.; Zhang, X. B.; Kong, R. M.; Yang, B.; Tan, W. H. *J. Am. Chem. Soc.* **2011***, 133*, 11686-11691.

(15) Paleček, E.; Bartošík, M. *Chem. Rev.* **2012**, *112*, 3427-3481.

(16) He, X.; Wang, G.; Xu, G.; Zhu, Y.; Chen, L.; Zhang, X. *Langmuir* **2013**, *29*, 14328-14334.

(17) Li, H.; Sun, Z.; Zhong, W.; Hao, N.; Xu, D.; Chen, H. Y. *Anal. Chem.* **2010**, *82*, 5477-5483.

(18) De La Escosura-Muniz, A.; Gonzalez-Garcia, M. B.; Costa-Garcia, A. *Biosens. Bioelectron.* **2007**, *22*, 1048-1054.

(19) Moreno-Hagelsieb, L.; Foultier, B.; Laurent, G.; Pampin, R.; Remacle, J.; Raskin, J. P.; Flandre, D. *Biosens. Bioelectron.* **2007**, *22*, 2199-2207.

(20) Wilner, O. I.; Willner, I. *Chem. Rev.* **2012**, *112*, 2528-2556.

(21) Lee, T. M. H.; Carles, M. C.; Hsing, I. M. *Lab Chip* **2003**, *3*, 100-105.

(22) Wang, F.; Lu, C. H.; Liu, X.; Freage, L.; Willner, I. *Anal. Chem.* **2014**, *86*, 1614-1621.

(23) Wang, C.; Zhou, H.; Zhu, W.; Li, H.; Jiang, J.; Shen, G.; Yu, R. *Biosens. Bioelectron.* **2013**, *47*, 324-328.

(24) Chen, X.; Lin, Y. H.; Li, J.; Lin, L. S.; Chen, G. N.; Yang, H. H. *Chem. Commun.* **2011**, *47*, 12116-12118.

(25) Liu, S.; Wang, C.; Zhang, C.; Wang, Y.; Tang, B. *Anal. Chem.* **2013**, *85*, 2282-2288.

(26) Chen, Y.; Jiang, B.; Xiang, Y.; Chai, Y.; Yuan, R. *Chem. Commun.* **2011**, *47*, 12798-12800.

(27) Zheleznaya, L. A.; Kachalova, G. S.; Artyukh, R. I.; Yunusova, A. K.;

Perevyazova, T. A.; Matvienko, N. I. *Biochemistry* **2009**, *74*, 1457-1466.

(28) Williams, R. J. *Mol. Biotechnol.* **2003**, *23*, 225-243.

(29) Kong, R. M.; Zhang, X. B.; Zhang, L. L.; Huang, Y.; Lu, D. Q.; Tan, W. H.; Shen, G. L.; Yu, R. Q. *Anal. Chem.* **2011**, *83*, 14-17.

(30) Kong, R. M.; Zhang, X. B.; Chen, Z.; Meng, H. M.; Song, Z. L.; Tan, W. H.; Shen, G. L.; Yu, R. Q. *Anal. Chem.* **2011**, *83*, 7603-7607.

(31) Chen, Y.; Wang, Q.; Xu, J.; Xiang, Y.; Yuan, R.; Chai, Y. *Chem. Commun.* **2013**, *49*, 2052-2054.

(32) Chen, J.; Zhang, J.; Guo, Y.; Li, J.; Fu, F.; Yang, H. H.; Chen, G. *Chem. Commun.* **2011**, *47*, 8004-8006.

(33) Lee, J. H.; Jang, H.; Cho, E. J.; Youn, H. D. *Biochem. Biophys. Res. Commun.* **2009**, *389*, 399-404.

(34) Chen, F.; Wang, W.; El-Deiry, W. S. *Biochem. Pharmacol.* **2010**, *80*, 724-730.

(35) Cheng, L. C.; Huang, J. H.; Chen, H. M.; Lai, T. C.; Yang, K. Y.; Liu, R. S.; Hsiao, M.; Chen, C. H.; Her, L. J.; Tsai, D. P. *J. Mater. Chem.* **2012**, *22*, 2244-2253.

(36) Zhang, H. J.; Toshima, N. *Catal. Sci. Technol.* **2013**, *3*, 268-278.

(37) Ksar, F.; Ramos, L.; Keita, B.; Nadjo, L.; Beaunier, P.; Remita, H. *Chem. Mater.* **2009**, *21*, 3677-3683.

(38) Gao, F.; Goodman, D. W. *Chem. Soc. Rev.* **2012**, *41*, 8009-8020.

(39) De Corte, S.; Hennebel, T.; Fitts, J. P.; Sabbe, T.; Bliznuk, V.; Verschuere, S.; van der Lelie, D.; Verstraete, W.; Boon, N. *Environ. Sci. Technol.* **2011**, *45*, 8506-8513.

(40) Shi, L. H.; Wang, A.Q.; Zhang, T.; Zhang, B. S.; Su, D. S.; Li, H. Q.; Song, Y. J. *J. Phys. Chem. C* **2013**, *117*, 12526-12536.

(41) Chen, C. H.; Sarma, L. S.; Chen, J. M.; Shih, S. C.; Wang, G. R.; Liu, D. G.;

Tang, M. T.; Lee, J. F.; Hwang, B. J. *ACS Nano* **2007**, *1*, 114-125.

(42) Nagaiah, T. C.; Schäfer, D.; Schuhmann, W.; Dimcheva, N. *Anal. Chem.* **2013**, *85*, 7897-7903.

(43) Li, Q.; Cui, C. C.; Higgins, D. A.; Li, J. *J. Am. Chem. Soc.* **2012**, *134*, 14467-14475.

(44) Kaiser, W.; Rant, U. *J. Am. Chem. Soc.* **2010**, *132*, 7935-7945.

(45) Yu, Z. G.; Lai, R. Y. *Anal. Chem.* **2013**, *85*, 3340-3346.

(46) Lane, D. P. *Nature* **1992**, *358*, 15-16.

(47) Riley, T.; Sontag, E.; Chen, P.; Levine, A. *Nat. Rev. Mol. Cell. Biol.* **2008**, *9*, 402-412.

(48) Bensaad, K.; Vousden, K. H. *Trends Cell Biol.* **2007**, *17*, 286-291.

(49) Kruse, J. P.; Gu, W. *Cell* **2009**, *137*, 609-622.

(50) Wang, X.; Zhang, X.; He, P.; Fang, Y. *Biosens. Bioelectron.* **2011**, *26*, 3608-3613.

(51) Luo, X.; Du, F.; Wu, Y.; Gao, L.; Li, X. *Chin. J. Anal. Chem.* **2013**, *41*, 11, 1664-1668.

(52) Hamidi-Asl, E.; Raoof, J. B.; Ojani, R.; Hejazi, M. S. *Electroanalysis* **2013**, *25*, 2075-2083.

(53) Li, H.; Wu, Z.; Qiu, L.; Liu, J.; Wang, C.; Shen, G.; Yu, R. *Biosens. Bioelectron.* **2013**, *50*, 180-185.

(54) Chen, J.; Zhang, J.; Guo, Y.; Li, J.; Fu, F.; Yang, H. H.; Chen, G. *Chem. Commun.* **2011**, *47*, 8004-8006.

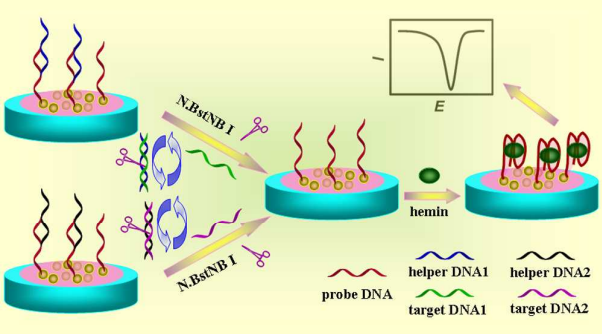
N.BstNB I
N.BstNB I
E
hemin
probe DNA
helper DNA1
target DNA1
helper DNA2
target DNA2

for TOC only